and

$$a(d-e)=0, \tag{B9}$$

but we are still unable to specify which factor of Eq. (B9) is zero.

Consideration of the process $\pi+\Lambda\rightarrow\pi+\Sigma$ leads to

$$p=0 \tag{B10}$$

and

$$bg=fd. \tag{B11}$$

The strangeness -1 amplitudes for $\bar{K}+N\rightarrow\pi+\Lambda$ lead to

$$kj=-il, \tag{B12}$$

while the process $\bar{K}+N\rightarrow\pi+\Sigma$ leads to

$$i^2=j^2, \tag{B13}$$

$$m^2=n^2=2k^2=2l^2, \tag{B14}$$

$$hin=gjm, \tag{B15}$$

and

$$\gamma' aml=\gamma c(k^2-l^2). \tag{B16}$$

Since $k^2=l^2$, the only solution to Eq. (B16) that allows any N-Σ coupling is

$$a=0, \tag{B17}$$

and then Eq. (B8) reduces to

$$e=-d. \tag{B18}$$

The relative magnitudes and sign correlations given by Eqs. (B1)–(B18) constitute charge independence for the meson-baryon coupling constants. Consideration of processes of the form $\pi+\text{baryon}\rightarrow\eta+\text{baryon}$ with a single neutral η meson then leads at once to isoscalar η coupling constants when the previously derived pion-coupling-constant relations are used. All processes that have not been explicitly considered in this Appendix are consistent with Eq. (2) but lead to no new information.

PHYSICAL REVIEW VOLUME 138, NUMBER 5B 7 JUNE 1965

Extrapolation of Nucleon Electromagnetic Form Factors*

J. S. LEVINGER† AND C. P. WANG‡
Cornell University, Ithaca, New York

(Received 21 December 1964)

We use conformal transformations to facilitate extrapolation of experimental values of the two isovector and two isoscalar nucleon form factors, to find their spectral functions. Both isovector spectral functions peak around 600 MeV, or somewhat below the energy of the isovector ρ resonance. Both isoscalar spectral functions peak around 700 MeV, somewhat below the ω resonance. We also analyze the electric form factor for elastic electron-deuteron scattering in terms of the difference between the measured value and the calculated value. The latter uses assumptions concerning the deuteron wave function, and concerning the isoscalar electric nucleon form factor G_{ES}. By extrapolating this difference, we find G_{ES} in the time-like region $t_A<t<9\mu_\pi^2$, where t_A is the anomalous threshold, and the upper limit is the normal isoscalar threshold. These values of G_{ES} are statistically consistent with the measurements for space-like momentum transfer. Extrapolation of the combined set of values for G_{ES} (space-like and time-like momentum transfers) gives a spectral function again peaking at 700 MeV, with indications of a dip at 1150 MeV. The dip may be due to the isoscalar ϕ resonance.

WE have previously used[1,2] a conformal transformation as a method to extrapolate the proton electric and magnetic form factors (G_{Ep} and G_{Mp}) measured for space-like momentum transfers to find the spectral function for time-like momentum transfers. Our basic equations and notations are given in the Appendix; see I and II for discussions and tests of our extrapolation techniques.

In this paper, we apply the same extrapolation techniques to measurements of the isovector and isoscalar nucleon electromagnetic form factors. We first use data,[3] compiled June 1964, on the neutron form factors found from inelastic electron-deuteron scattering and also from scattering of thermal neutrons. The procedure is straightforward: We merely combine these neutron form factors with proton form factors at the same space-like momentum transfer to find the isovector and isoscalar form factors, which we then extrapolate. The

* A preliminary account was communicated to the Eastern Theoretical Physics Conference, Washington, D. C., October 1964. This work was supported in part by the U. S. Office of Naval Research.

† AVCO Visiting Professor; present address: Rensselaer Polytechnic Institute, Troy, New York.

‡ Present address: Catholic University of America, Washington, D. C.

[1] J. S. Levinger and R. F. Peierls, Phys. Rev. **134**, B1341 (1964), referred to as I. See this paper for further references to the literature.

[2] J. S. Levinger and C. P. Wang, Phys. Rev. **136**, B733 (1964), referred to as II.

[3] R. R. Wilson and J. S. Levinger, Ann. Rev. Nucl. Sci. **14**, 135 (1964).

TABLE I. Input data. η is given by Eq. (A2). The nucleon electric (E) and magnetic (M) isoscalar (S) and isovector (V) form factors are taken from Ref. 3.

		Isovector form factors			
t (F^{-2})	η	G_{MV}	Error	G_{EV}	Error
−1	0.240	...	...	0.430	0.007
−4.9	0.037	1.375	0.065	0.225	0.020
−10	−0.101	0.965	0.030	0.193	0.036
−10	−0.101	...	...	0.133	0.030
−11	−0.121	0.905	0.060	0.108	0.090
−12	−0.138	0.875	0.030	0.146	0.046
−14	−0.172	0.780	0.030	0.135	0.036
−15	−0.186	0.715	0.050	0.140	0.080
−16	−0.206	0.680	0.015	0.107	0.030
−20	−0.248	0.520	0.045	0.085	0.070
−25	−0.295	0.370	0.040	−0.005	0.080
−30	−0.333	0.340	0.020	−0.028	0.018
−35	−0.366	0.160	0.080	−0.068	0.060
−45	−0.416	0.227	0.013	0.006	0.036
−75	−0.512	0.080	0.030	−0.010	0.040
$-\infty$	−1.000	0.000	0.030	0.000	0.040
		Isoscalar form factors			
t (F^{-2})	η	G_{MS}	Error	G_{ES}	Error
−1	0.288	...	...	0.450	0.007
−4.9	0.160	0.315	0.065	0.385	0.020
−10	0.054	0.185	0.030	0.243	0.036
−10	0.054	...	...	0.303	0.030
−11	0.037	0.165	0.060	0.298	0.090
−12	0.022	0.125	0.030	0.240	0.046
−14	−0.008	0.120	0.030	0.205	0.036
−15	−0.020	0.125	0.050	0.180	0.080
−16	−0.033	0.110	0.015	0.190	0.030
−20	−0.077	0.130	0.045	0.165	0.070
−25	−0.123	0.130	0.040	0.200	0.080
−30	−0.161	0.060	0.020	0.183	0.018
−35	−0.195	0.160	0.080	0.193	0.060
−45	−0.248	0.013	0.013	0.085	0.036
−75	−0.356	0.025	0.030	0.050	0.040
$-\infty$	−1.000	0.000	0.030	0.000	0.040

spectral functions determined in this manner might well have simple interpretations in terms of resonant intermediate 1^- states of definite isospin: e.g., the isovector ρ, and the isoscalar ω and ϕ. The magnetic isovector spectral function has been determined by Zeiler[4] in a similar manner, and we shall compare with his results.

We then analyze electron-deuteron elastic scattering (electric form factor G_{Ed}) to determine in a second manner the electric isoscalar nucleon form factor, G_{ES}. Previous work[5–8] used the measurements to determine G_{ES} for space-like momentum transfers and found values inconsistent with those based on scattering of thermal neutrons. We extrapolate the measurements of G_{Ed} to time-like momentum transfers in the interval between the deuteron's anomalous threshold of $1.73\ \mu_\pi^2$ and the normal isoscalar threshold of $9\ \mu_\pi^2$. (Here μ_π is the pion mass.) We find that our values for G_{ES} in this region are consistent with values of G_{ES} for space-like momentum transfer. Thus, our new method of analyzing elastic electron-deuteron scattering seems to remove the inconsistency between G_{ES} found from elastic and inelastic scattering measurements.

II. EXTRAPOLATION OF ISOVECTOR AND ISOSCALAR FORM FACTORS

The isovector magnetic and electric form factors are related to the proton (p) and neutron (n) form factors in the standard manner:

$$G_{MV}=\tfrac{1}{2}(G_{Mp}-G_{Mn}),$$
$$G_{EV}=\tfrac{1}{2}(G_{Ep}-G_{En}). \quad (1)$$

We use as input data the magnetic and electric neutron form factors G_{Mn} and G_{En} given in Fig. 7 of Wilson and Levinger.[3,9] (Note that these values are as of June 1964. Table II of Wilson-Levinger is based on slightly later measurements[10]; these new data would not substantially alter our results.) These data from inelastic electron-deuteron scattering measure $(G_{Mn})^2$ and $(G_{En})^2$ and thus do not give the signs of G_{Mn} or G_{En}. We assume the signs as negative for the former and positive for the latter. Our assumption for the sign of G_{En} is based on the measured electron-neutron scattering length,[11] which gives

$$dG_{En}/dq^2|_0=0.021\ \text{F}^2. \quad (2)$$

We also use Eq. (2) to give us a value for G_{En} at $t=-q^2=-1$ F^{-2}, namely $G_{En}=0.02$.

The values for proton form factors are taken from Wilson and Levinger's compilation, interpolating where necessary. The errors for G_{MV} and G_{EV} are almost entirely due to the errors in the neutron form factors; we use the errors given by the experimentalists.

Our input data for the isovector form factor is given in Table I. Note that we use normalizations $G_{MV}(0)=2.353$, and $G_{EV}(0)=\frac{1}{2}$. We also give the value of η

TABLE II. Goodness of fit versus degree of polynomial. Here $\phi=\chi^2/$(degrees of freedom), for a polynomial of degree N with two constraints, fitting data of Table I.

N	ϕ for G_{MV}	ϕ for G_{EV}	ϕ for G_{MS}	ϕ for G_{ES}
3	2.01	1.10	2.35	1.45
4	1.37	1.18	0.77	1.08
5	1.18	1.17	0.85	1.02

[4] J. Zeiler, Diplomarbeit, Technische Hochschule, Karlsruhe, Germany, 1963 (unpublished).
[5] N. K. Glendenning and G. Kramer, Phys. Rev. Letters **7**, 471 (1961); Phys. Rev. **126**, 2159 (1962); J. I. Freidman, H. W. Kendall, and P. A. M. Gram, *ibid.* **120**, 992 (1960).
[6] D. J. Drickey and L. N. Hand, Phys. Rev. Letters **9**, 521 (1962).
[7] B. Grossetête and P. Lehmann, Nuovo Cimento **28**, 423 (1963).
[8] D. Benaksas, D. Drickey, and D. Frèrejacque, Phys. Rev. Letters **13**, 353 (1964); and D. Benaksas (private communication).
[9] T. A. Griffy, R. Hofstadter, E. B. Hughes, T. Janssens, and M. R. Yearian, Dubna Conference (unpublished); C. Akerlof, K. Berkelman, G. Rouse, and M. Tigner, Phys. Rev. **135**, B810 (1964); J. R. Dunning (private communication); P. Stein, R. W. McAllister, B. D. McDaniel, and W. M. Woodard, Phys. Rev. Letters **9**, 403 (1962).
[10] J. R. Dunning, K. W. Chen, A. A. Cone, G. Hartwig, N. F. Ramsey, J. K. Walker, and Richard Wilson, Phys. Rev. Letters **13**, 631 (1964).
[11] L. L. Foldy, Rev. Mod. Phys. **30**, 471 (1958).

TABLE III. Coefficients a_n, and diagonal errors, for polynomial fits to data of Table I.

	G_{MV}(quartic)		G_{MV}(quintic)		G_{EV}		G_{MS}		G_{ES}	
n	a_n	Error	a_n	Error	a_n	Error	a_n	Error	a_n	Error
0	1.258	0.013	1.305	0.029	0.229	0.007	0.136	0.010	0.241	0.010
1	3.097	0.013	3.329	0.130	0.783	0.017	0.662	0.029	0.628	0.042
2	0.976	0.124	0.489	0.299	0.208	0.026	0.849	0.144	0.530	0.160
3	−1.149	0.032	−3.227	1.159	−0.352	0.021	−0.152	0.058	−0.158	0.074
4	−0.285	0.095	−0.185	0.110	···	···	−0.476	0.107	−0.304	0.123
5	···	···	1.506	0.840	···	···	···	···	···	···

used in our conformal transformation, for a threshold, t_0 of 4 squared pion masses, and $b=2$. [See Eq. (A2) for notation.] We are assuming a nonsubtracted dispersion relationship, to good accuracy; that is, we assume that G_{MV} and G_{EV} at infinite space-like momentum transfer are each zero, and we assign errors for this "datum" as the same as for the measurements at $t=-75$ F^{-2}. Table I also gives the input data for isoscalar form factors.

Table II gives the goodness of fit ϕ for the input data of Table I, when we fit with a polynomial of degree N (with two constraints) in the variable η. The quantity $\phi=\chi^2/$(degrees of freedom) should be close to unity. Using Table II, we choose a quintic fit for the isovector magnetic form factor G_{MV}, and a cubic fit for the isovector electric form factor G_{EV}. We also include a quartic fit to G_{MV} for comparison. The isoscalar form factors G_{MS} and G_{ES} are each fitted by quartics.

TABLE IV. Form factors for real η, using the coefficients of Table III, and the complete error matrix for the statistical error. See Eqs. (A2) and (A3).

		Isovector					
		Quartic		Quintic		Cubic	
η	t(F^{-2})	G_{MV}	Error	G_{MV}	Error	G_{EV}	Error
0.92	1.99	3.83	0.04	3.13	0.40	0.85	0.01
0.80	1.90	3.66	0.04	3.05	0.34	0.81	0.01
0.68	1.71	3.39	0.03	2.96	0.24	0.747	0.007
0.56	1.26	3.07	0.02	2.82	0.14	0.671	0.005
0.44	0.79	2.70	0.01	2.61	0.05	0.584	0.002
0.333	0.00	2.353	0.000	2.353	0.000	0.500	0.000
0.32	−0.12	2.309	0.001	2.317	0.005	0.4893	0.0003
0.20	−1.56	1.91	0.01	1.96	0.03	0.391	0.003
0.08	−3.78	1.51	0.01	1.57	0.04	0.293	0.005
−0.04	−7.38	1.14	0.01	1.17	0.02	0.198	0.007
−0.16	−13.2	0.79	0.01	0.80	0.01	0.11	0.01
−0.28	−23.2	0.49	0.01	0.48	0.01	0.03	0.01
−0.40	−41.5	0.24	0.01	0.24	0.01	−0.03	0.01
−0.52	−78.1	0.05	0.02	0.09	0.03	−0.07	0.01
−0.64	−180	−0.07	0.02	0.03	0.06	−0.09	0.02
−0.76	−427	−0.12	0.02	0.03	0.09	−0.09	0.02
−0.88	−1958	−0.10	0.02	0.05	0.08	−0.06	0.03
−1.00	−∞	0.00	0.03	0.00	0.03	0.01	0.04

		Isoscalar			
η	t(F^{-2})	G_{MS}	Error	G_{ES}	Error
0.92	4.48	1.00	0.06	0.93	0.06
0.80	4.28	0.94	0.05	0.88	0.05
0.68	3.85	0.83	0.04	0.80	0.04
0.56	2.84	0.70	0.02	0.70	0.02
0.44	1.78	0.56	0.01	0.60	0.01
0.333	0.00	0.440	0.000	0.500	0.000
0.32	−0.27	0.425	0.001	0.488	0.001
0.20	−3.51	0.30	0.01	0.39	0.01
0.08	−8.50	0.19	0.01	0.29	0.01
−0.04	−16.6	0.11	0.01	0.22	0.01
−0.16	−29.7	0.05	0.01	0.15	0.01
−0.28	−52.4	0.02	0.01	0.11	0.02
−0.40	−93.4	0.01	0.02	0.08	0.03
−0.52	−176.	0.01	0.03	0.06	0.04
−0.64	−405.	0.02	0.04	0.05	0.05
−0.76	−961	0.03	0.04	0.04	0.05
−0.88	−4406	0.03	0.03	0.03	0.04
−1.00	−∞	0.00	0.03	0.00	0.04

TABLE V. Spectral functions, using coefficients of Table III, and the complete error matrix. See Eqs. (A4) and (A5).

Isovector

ξ (deg)	Mass (MeV)	Quartic g_{MV}	Quartic Error	Quintic g_{MV}	Quintic Error	Cubic g_{EV}	Cubic Error
0.0	280	0.00	0.00	0.00	0.00	0.00	0.00
14.9	289	0.21	0.003	0.13	0.04	0.05	0.001
25.8	308	0.70	0.03	−0.32	0.57	0.16	0.004
37.3	337	1.59	0.09	−0.77	1.32	0.35	0.01
47.5	373	2.61	0.15	−0.25	1.61	0.57	0.02
58.1	418	3.61	0.18	1.65	1.11	0.81	0.03
66.1	459	4.19	0.17	3.84	0.27	0.98	0.04
74.6	509	4.53	0.13	6.15	0.91	1.10	0.04
83.3	571	4.51	0.05	7.79	1.83	1.16	0.04
89.9	622	4.27	0.04	8.07	2.12	1.14	0.03
96.1	683	3.85	0.10	7.49	2.04	1.07	0.03
104.	757	3.26	0.15	6.05	1.56	0.95	0.02
106.	800	2.93	0.18	5.06	1.20	0.87	0.02
114	903	2.20	0.20	2.81	0.39	0.68	0.02
122	1037	1.46	0.19	0.63	0.50	0.46	0.02
126	1120	1.11	0.17	−0.26	0.78	0.34	0.03
129	1217	0.78	0.15	−0.94	0.97	0.23	0.03
134	1333	0.49	0.12	−1.38	1.06	0.13	0.04
138	1474	0.25	0.09	−1.58	1.02	0.04	0.04
142	1647	0.05	0.06	−1.55	0.89	−0.04	0.04
147	1867	−0.11	0.04	−1.34	0.69	−0.10	0.04
151	2154	−0.21	0.03	−1.02	0.45	−0.15	0.04
155	2545	−0.27	0.04	−0.67	0.22	−0.17	0.04
160	3111	−0.28	0.04	−0.34	0.05	−0.17	0.03
164	4000	−0.26	0.04	−0.09	0.11	−0.16	0.03
168	5600	−0.21	0.04	0.05	0.15	−0.12	0.02
180	∞	0.00	0.00	0.00	0.00	0.00	0.00

Isoscalar

ξ (deg)	Mass (MeV)	Quartic g_{MS}	Quartic Error	Quartic g_{ES}	Quartic Error
0.0	420	0.00	0.00	0.00	0.00
14.9	434	0.07	0.01	0.05	0.01
25.8	462	0.34	0.05	0.24	0.06
37.3	506	0.83	0.12	0.58	0.13
47.5	560	1.33	0.18	0.95	0.20
58.1	627	1.68	0.20	1.23	0.22
66.1	688	1.76	0.17	1.32	0.19
74.6	764	1.60	0.11	1.26	0.12
83.3	856	1.21	0.03	1.03	0.04
89.9	933	0.84	0.08	0.80	0.11
96.1	1024	0.43	0.15	0.54	0.19
104.	1136	0.02	0.22	0.27	0.26
106.	1200	−0.16	0.24	0.14	0.28
114	1354	−0.45	0.25	−0.07	0.30
122	1556	−0.59	0.23	−0.19	0.27
126	1680	−0.60	0.21	−0.22	0.24
129	1826	−0.57	0.18	−0.23	0.20
134	2000	−0.52	0.14	−0.21	0.16
138	2211	−0.43	0.10	−0.18	0.11
142	2470	−0.33	0.06	−0.13	0.07
147	2800	−0.23	0.03	−0.08	0.04
151	3231	−0.13	0.03	−0.03	0.05
155	3818	−0.05	0.05	0.01	0.06
160	4666	0.01	0.06	0.03	0.07
164	6000	0.05	0.06	0.05	0.07
168	8400	0.06	0.05	0.05	0.06
180	∞	0.00	0.00	0.00	0.00

Table III gives the coefficients a_n and diagonal errors for the polynomials as selected in the above paragraph. These coefficients, and the complete error matrix, are used to give the form factors for real values of η presented in Table IV. Here the values for $-75<t<0$ are interpolations of the input data of Table I; while the remainder of Table IV gives extrapolations. Note that the extrapolated values for G_{MV} for $t<-75$ F^{-2} appear rather different for the quartic and quintic fits. However, the difference is only about two statistical errors, due to the large error of the quintic fit, so it should not be taken seriously. Similarly, the statistical errors given in Table IV for the quartic fit to G_{MV} are unrealistically small in this region of momentum transfer. They represent the error only if we assume that we *must* fit with a quartic. Since the statistical criterion given in Table II does not demand a quartic fit, but in fact suggests a quintic fit, the statistical error *assuming* a quartic fit does not include the main source of error.

Table V gives the spectral functions, and their statistical errors, for the coefficients of Table III. We also compare three different isovector magnetic spectral functions in Fig. 1: the quartic and quintic from Table V, and Zeiler's[4] third spectral function in his Fig. 13(b). [This fit of Zeiler's uses a quartic, with an unsubtracted dispersion relation and constraint (A6). Zeiler here uses $b=2.2$, very nearly the value of 2.0 that we have taken.] The figure shows that all three spectral functions peak in the region of 600 MeV: namely, 500, 620, and 620 MeV for our quartic, quintic, and Zeiler's fits, respectively. The full width at half-maximum Γ is 530, 360, and 620 MeV for the three fits. It is more meaningful to express the width Γ in terms of the angle in the η plane: namely, 68, 42, and 66°, respectively. Our work in I shows that a very narrow peak fitted by a polynomial of degree N will have a width of about $180/N$ in angle ξ. Since Fig. 1 gives somewhat larger values, there is a *suggestion* that the true spectral function may have a nonzero width, or may have structure. The position of the peak is lower, in each case, than the 750 MeV shown in Fig. 1 for the center of the ρ resonance; but it is not clear whether this difference is significant. It is significant that we obtain a peak near 750 MeV for the isovector spectral function without at any time assuming that the spectral function should have a peak in this region. We used only knowledge of the isovector threshold and of the zero slope of the spectral function at threshold. See I for further discussion and tests of the significance of spectral function peaks found by our extrapolation technique.

There is a slight tendency for the magnetic isovector spectral function to become negative for high values of the mass of the intermediate state; this tendency is weak compared to the rather definite negative peak around 1500 MeV for the proton spectral functions found in II.

We should make clear that we have selected one of many extrapolations made by Zeiler. In fact, the main point that he makes is that this extrapolation procedure has two arbitrary features. First, he obtains different results for different values of the degree N of the polynomial chosen; second, he obtains different results for different choices of the parameter b in Eq. (A2). We argue that the choice of N is actually not arbitrary but, in fact, is determined by statistical criteria, as illustrated in Table II. A possible uncertainty between neighboring integers for values of N does not cause great difficulties, particularly when one considers the large statistical errors in the fit with the larger value of N, as is done in Fig. 1. (Zeiler does not use the original experimental errors in his input data, and does not make an error analysis of the output spectral function.) In II, we discuss the dependence on the parameter b, and we justify the choice $b=2$ for fitting

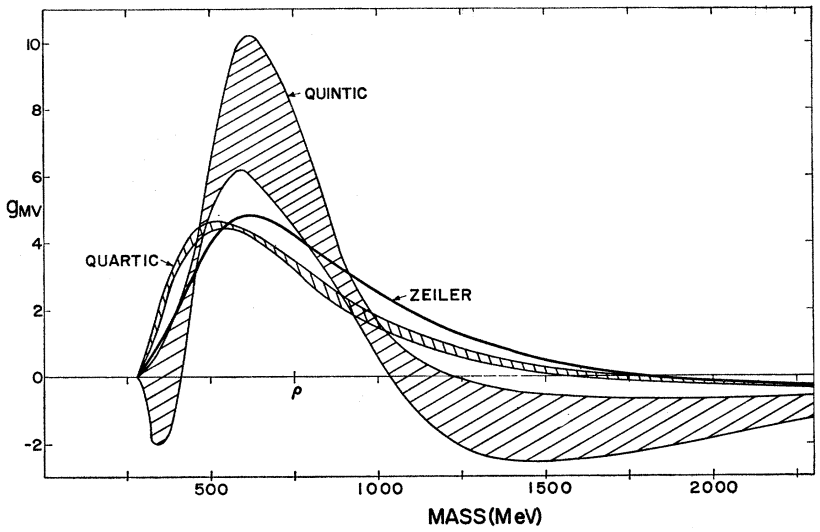

FIG. 1. Magnetic isovector spectral function plotted versus mass in MeV. The curve marked "Zeiler" is from Ref. 3, using Zeiler's third spectral function in his Fig. 13(b). Our quartic and quintic fits, with their statistical errors, are taken from Table V.

proton form factors. The value of b is not as definite for the isovector form factors; but we believe that b should not be allowed to vary over the *wide* range used by Zeiler. Correspondingly, the effect of varying b will not greatly affect the main features of the spectral function. [See Fig. 6(b) of II: A change of $\frac{1}{2}$ in b changes the peak energy by less than 100 MeV.]

Table V shows that the isovector electric spectral function g_{EV} behaves similarly to the magnetic g_{MV}. The peak of the electric spectral function is at 580 MeV, in the region of the three fits discussed above for g_{MV}. The width of 600 MeV, or 60° in ξ is to be expected for a cubic fit to a resonance much narrower than 600 MeV. There is an indication of a minimum of the electric spectral function around 2500 MeV.

The isoscalar spectral functions g_{MS} and g_{ES} also given in Table V each peak around 690 MeV, or somewhat lower than the 790-MeV position of ω resonance. Again a peak in the right region has been found directly from the data and knowledge of the threshold behavior alone. There is an indication (3 standard errors) of a minimum around 1700 MeV. The width of 420 MeV, or 50° for the main peak is consistent with quartic fits to a narrow resonance.

So far we have neglected the condition used in II that the complex magnetic and electric form factors should be equal at $t=4M^2$, where M is the nucleon mass. Table VI shows that this condition is in fact met, within statistical errors, by our extrapolations.

TABLE VI. Values of nucleon form factors at $t=4M^2$. Form factors and statistical errors using coefficients of Table III. The corresponding magnetic and electric form factors are not inconsistent with each other, in a statistical sense, at $t=4M^2$.

	Magnetic	Electric
Real part of isovector:	(quartic) -0.96 ± 0.11	-0.41 ± 0.19
	(quintic) -0.30 ± 0.39	
Imaginary part, isovector:	(quartic) -0.11 ± 0.04	-0.10 ± 0.04
	(quintic) $-1.3\ \pm0.7$	
Real part, isoscalar	-0.10 ± 0.13	-0.10 ± 0.17
Imaginary part, isoscalar	-0.55 ± 0.17	-0.22 ± 0.20

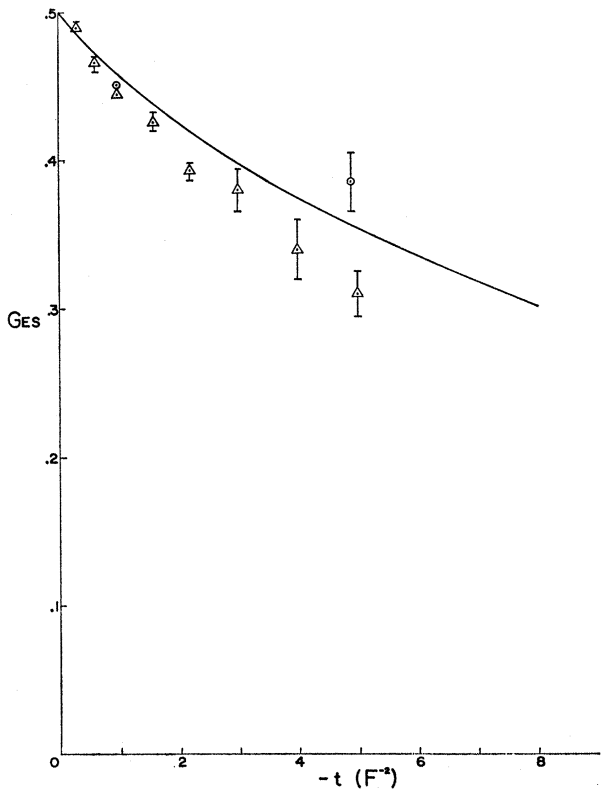

FIG. 2. The isoscalar electric form factor G_{ES} versus q^2 in F^{-2}. The circles from Table I are based on inelastic electron-deuteron scattering, and on scattering of thermal neutrons; the triangles from Refs. 6 and 8 are based on elastic electron-deuteron scattering; the curve from Table IV is our interpolation for the data of Table I.

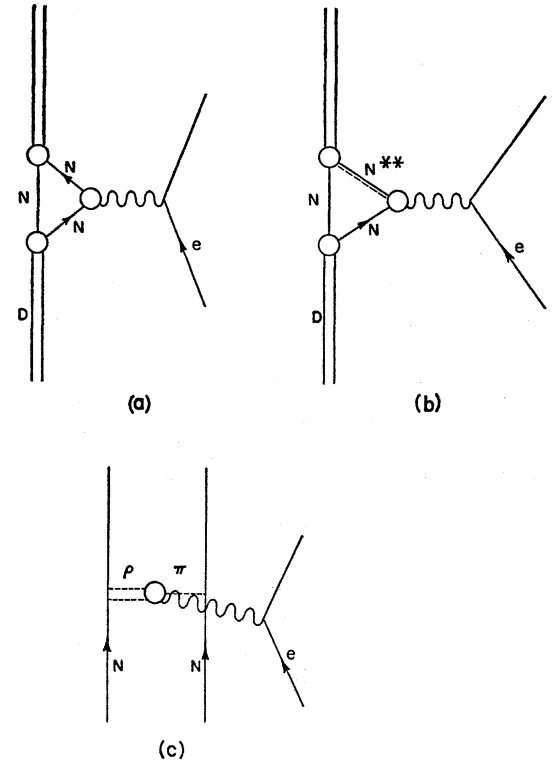

FIG. 3. Diagrams for elastic electron-deuteron scattering. (a) is the additive diagram, with anomalous threshold $1.73\,\mu_\pi{}^2$; while (b) and (c) represent two of the infinite number of nonadditive diagrams.

III. ELECTRON-DEUTERON ELASTIC SCATTERING

As we have mentioned briefly in the Introduction, previous analyses of electron-deuteron elastic scattering give results for G_{ES} for space-like momentum transfers which are inconsistent with those used in our input data, Table I. The disagreement is illustrated in Fig. 2, where we show use of the analysis of Drickey *et al.*[6,8] as triangles, compared to circles from Table I and the solid curve from Table IV. (This disagreement is usually shown in a more striking manner by comparing values for the neutron electric form factor G_{En}. In either case, the disagreement is statistically significant.) We note again that the "datum point" for $t=-1$ F^{-2} is based on scattering of thermal neutrons, while we have assumed a positive sign for G_{En} for the point at $t=-4.9$ F^{-2}.

In this paper, we shall instead analyze the region

$$t_A\leq t\leq 9\mu_\pi{}^2;\quad 0.865\text{ F}^{-2}\leq t\leq 4.5\text{ F}^{-2}. \tag{3}$$

Here $t_A=1.73\,\mu_\pi{}^2$ is the anomalous threshold for the deuteron, while $9\mu_\pi{}^2$ is the normal threshold for an isoscalar intermediate state. In the region of Eq. (3), we have the special feature that the imaginary part of the deuteron form factor[12] is accurately known from effective-range theory, and that the nucleon isoscalar form factor G_{ES} is real. We use the notation

$$G_{Ed}=2DG_{ES}+R. \tag{4}$$

Here G_{Ed} is the electric form factor (including quadrupole effects) for elastic electron-deuteron scattering. D is the quantity which in a nonrelativistic theory is the Fourier transform of the squared wave function of the deuteron, and therefore, in a relativistic theory,[12] has become complex at the anomalous threshold $t_A=16M\epsilon=0.865$ F^{-2}. (Here M is the proton mass and ϵ is the binding energy of the deuteron.) R stands for all "nonadditive" terms. Figure 3(a) illustrates the additive term $2DG_{ES}$; Figs. 3(b) and (c) illustrate two of the many nonadditive terms. Of course, $R=0$ for $t=0$, from charge conservation, while for the magnetic analog of Eq. (4) the nonadditive term may be of significance even in the static limit.[13] The usual procedure[5–8] is to assume a value for D, and assume R is zero for the space-like momentum transfers at which G_{Ed} is measured.

Our procedure has two main advantages over the usual procedure of assuming an expression for D and assuming $R=0$. First, we treat the problem relativistically. Second, we make a minimum of assumptions concerning the neutron-proton potential: We use the deuteron binding energy and the triplet effective range. In contrast, the usual use[5–8] of the nonrelativistic Hamada-Johnston wave function to give $D(t)$ for space-like t involves the assumption that a static potential should be used to extrapolate from neutron-proton scattering to find the off-energy-shell matrix elements involved in D. (Of course, properties of the deuteron ground state are used to constrain the extrapolation.) But how do we know that the neutron-proton potential is not velocity-dependent at small distances? Further, the customary neglect[5–8] of nonadditive terms R in Eq. (4) is justified only by the resulting simplification of the calculation. Since R is expected to decrease less rapidly than D with large space-like increasing q^2, we do not see why R should be neglected. Indeed, our analysis below *suggests* that R/D is *not* negligible at moderate space-like momentum transfers, e.g., $t=-5$ F^{-2}. Here the Hamada-Johnston wave function gives $D=0.204$; using $R=0$ and the measured $G_{Ed}=0.125$ gives $G_{ES}=0.31$, which is plotted as a triangle in Fig. 2. We find from our analysis (Table XII and Fig. 5): $G_{ES}=0.346$, and $R=-0.016$. Thus R is small compared to unity, but R is almost 10% of D at this momentum transfer, *if* we use D for the Hamada-Johnston wave function.

We fit the data for space-like momentum transfer with the expression

$$G_{Ed}=JG-Y. \tag{5}$$

We choose a form for J which has an imaginary part

[12] F. Gross, Phys. Rev. **134**, B405 (1964); **146**, B140 (1964).

[13] D. Harrington, Phys. Rev. **133**, B142 (1964); A. Q. Sarker, Phys. Rev. Letters **13**, 375 (1964) and (private communication); R. J. Adler and S. D. Drell, Phys. Rev. Letters **13**, 349 (1964).

TABLE VII. Electron-deuteron elastic scattering. The quantities Y given in the last four columns are found from (Eq. 5) using different choices [(8a), (8b), (7) and related material] for J and G, respectively.

		Input data			Two-pole G		One-pole G	
t(F^{-2})	η	G_{Ed}	Error	Ref.	Hulthén	Hamada	Hulthén	Hamada
−0.3	0.265	0.824	0.006	a	−0.002	−0.004	−0.002	−0.005
−0.6	0.212	0.680	0.004	a	0.016	0.011	0.016	0.010
−0.882	0.169	0.599	0.009	b	0.007	−0.001	0.007	−0.001
−1.002	0 153	0.546	0.004	a,b	0.027	0.017	0.028	0.016
−1.334	0.113	0.472	0.009	b	0.025	0.010	0.026	0.011
−1.590	0.086	0.429	0.006	a	0.019	0.003	0.021	0.005
−2.28	0.024	0.319	0.010	a,c	0.031	0.010	0.033	0.012
−3.0	−0.028	0.255	0.007	d	0.026	0.000	0.029	0.003
−3.2	−0.041	0.219	0.012	c	0.044	0.018	0.047	0.020
−3.96	−0.083	0.162	0.009	c	0.051	0.026	0.054	0.027
−4.0	−0.085	0.174	0.005	d	0.036	0.010	0.040	0.013
−4.93	−0.129	0.148	0.008	c	0.018	−0.009	0.023	−0.006
−5.0	−0.131	0.125	0.003	d	0.039	0.012	0.041	0.015
−6.0	−0.170	0.093	0.005	e	0.037	0.011	0.042	0.012

[a] Drickey and Hand, Ref. 6.
[b] Grosstête and Lehmann, Ref. 7.
[c] Friedman *et al.*, Ref. 5, as analyzed by M. Casper (private communication).
[d] Benaksas, Drickey, and Frèrejacque, Ref. 8.
[e] Benaksas (private communication).

equal to ImD in the region of Eq. (3): This means that J and D should have the same value for the effective range $\rho(-\epsilon,-\epsilon)$, since in this region

$$\mathrm{Im}J=\mathrm{Im}D=\tfrac{1}{2}\pi(1-\alpha\rho)^{-1}(t_A/t)^{1/2}. \quad (6)$$

[The value given for ImD depends just on the coefficient of $\exp(-\alpha r)$ in the deuteron wave function; and this coefficient is determined by the values of α and ρ.] In this paper, we make two specific choices of J, corresponding to a central Hulthén potential, and corresponding to a Hamada-Johnston potential.[6,8] Both use $\rho=1.76$ F and are illustrated for negative t in Fig. 4. The Hulthén choice for J has a simple analytical expression:

$$J(q)=(1.565/q)[\cot^{-1}(0.9268/q) +\cot^{-1}(5.508/q)-2\cot^{-1}(3.217/q)]. \quad (7)$$

Note $q=(-t)^{1/2}$ is positive for space-like momentum transfer.

We choose G to be similar to $2G_{ES}$ in the following respects: (i) static value of unity; (ii) slope dG/dt evaluated at t of zero should be 0.09 F^{-2}, based on $e-p$ scattering, and scattering of thermal neutrons; (iii) G goes to zero as t goes to infinity; (iv) Im$G=0$ for $t<t_0=4.5$ F^{-2}. We have used both one-pole and two-pole Clementel-Villi forms for G, namely,

$$G_1=11/(11-t), \quad (8a)$$

$$G_2=33.9/(16-t)-30.2/(27-t). \quad (8b)$$

In the one-pole expression we have no freedom as to the position of the pole; the position of 11 F^{-2} is below that of the observed isoscalar resonances. In the two-pole expression we have chosen the pole positions to correspond to the ω and ϕ resonances.

For each of these choices of J and G, we determine Y using experimental values of G_{Ed} for negative t. We make conformal transformation (A2) using $t_0=0.865$ F^{-2} and $b=2$, so that Y has, in general, a nonzero imaginary part in the region of Eq. (3). Equating the imaginary parts of Eqs. (4) and (5) and using (6), we

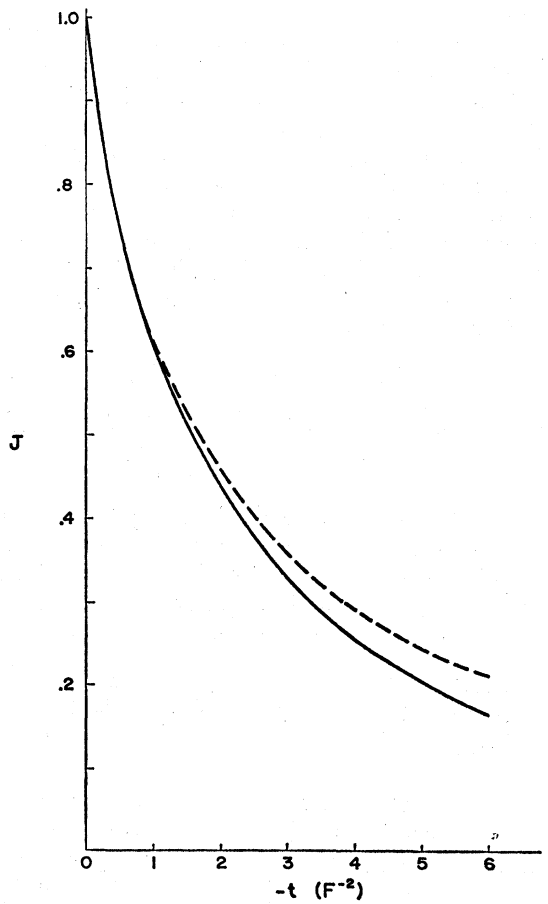

FIG. 4. The deuteron form factor J versus q^2 in F^{-2}. The dashed curve for a Hulthén potential is taken from Eq. (7); while the solid curve for a Hamada-Johnston potential is taken from Refs. 6 and 8.

TABLE VIII. Goodness of fit versus degree of polynomial. The goodness of fit is given by $\phi=\chi^2/(\text{degrees of freedom})$. The values of Y given in Table VII are fitted by polynomials in η with three constraints.

	Two-pole G		One-pole G	
N	Hulthén J	Hamada-Johnston	Hulthén J	Hamada-Johnston
2	28.5	4.5	33.0	5.1
3	1.75	1.75	1.84	1.46
4	1.65	1.77	1.55	1.55
5	1.79	1.89	1.69	1.70

find

$$G_{ES}=\tfrac{1}{2}G-\mathrm{Im}Y/2\,\mathrm{Im}D. \tag{9}$$

We used Eq. (5) after several attempts to extrapolate G_{Ed} into region (3). For example, M. Casper extrapolated G_{Ed} directly, using the anomalous threshold. He found a spectral function which rose quite rapidly for $t>t_A$. However, this technique could not give a spectral function which *jumps* from zero for $t<t_A$ to the value $\pi G_{ES}(t_A)(1-\alpha\rho)^{-1}$ for $t>t_A$. This jump cannot be reproduced accurately by a Fourier series truncated after several terms.

By extrapolating Y, defined in Eq. (5), we obviate this difficulty since $\mathrm{Im}Y=0$ for $t<t_A$ and starts at 0 for $t>t_A$. [Here we assume that Eq. (6) is satisfied and also that $G(t_A)=2G_{ES}(t_A)$.]

In other words, by introducing J we are making full use of our knowledge of the deuteron's spectral function: We use *both* the value of the anomalous threshold *and* the value of the jump at that threshold. We can then hope to find the value of G_{ES} in region (3).

We use three constraints on the polynomial in η. The static value $Y(0)=0$ gives

$$\Sigma_n a_n[(b-1)/(b+1)]^n=0. \tag{10}$$

The condition that $tY(t)$ remain finite for $t=-\infty$ gives

$$\Sigma_n(-1)^n a_n=\Sigma_n(-1)^n n a_n=0. \tag{11}$$

The above analysis is applied here only to the electric form factor G_{Ed} for electron-deuteron elastic scattering; the deuteron has a form factor G_c associated with the electric monopole, and a form factor G_Q for the electric quadrupole. Present measurements for unpolarized deuterons determine $G_{Ed}=[G_c^2+(t^2/18M^4)G_Q^2]^{1/2}$. The magnetic form factor of the deuteron has been measured but with less accuracy than the electric form factor, so in this paper we limit our work to G_{Ed}. The input data for the electric form factor and its statistical error is given in Table VII. Four values of Y are given, using choice (8a) or (8b) for G; and with a Hulthén choice, Eq. (7) for J, or a value of J for a Hamada-Johnston potential. Of course, the error in Y is the same as that in G_{Ed}.

TABLE IX. Coefficients for fits of polynomial (with three constraints) to values of Y given in Table VII. Quartic fits are given for a Hulthén choice for J; and cubic fits for a Hamada-Johnston choice for J.

	Two-pole G		One-pole G	
	Hulthén J	Hamada-Johnston	Hulthén J	Hamada-Johnston
0	0.032	0.011	0.034	0.012
1	−0.055	−0.011	−0.065	−0.012
2	−0.136	−0.053	−0.140	−0.062
3	0.019	−0.032	0.053	−0.037
4	0.069	···	0.093	···

Table VIII is used to determine the degree N of the extrapolating polynomials. We find that we should use a cubic for either G for a Hamada-Johnston choice for J and a quartic for a Hulthén choice for J. (Our choice of a quartic rather than a cubic for Hulthén J is controversial.)

The coefficients of Table IX are used to determine $\mathrm{Im}Y$ in the region of Eq. (3). The complete error matrix is used to determine the statistical error in $\mathrm{Im}Y$. These values of $\mathrm{Im}Y$ are then substituted into Eq. (9) to determine the isoscalar nucleon form factor G_{ES} in this region. [The value of G is taken from Eqs. (8a) and (8b), and $\mathrm{Im}D$ from Eq. (6).] Our results are given in Table X. It is clear that there is some dependence on the choices made for G and J. The dependence on J is not far outside the purely statistical errors; the dependence on G is statistically significant for a Hamada-Johnston choice for J. It would, therefore, be unrealistic to have confidence in the very small errors given in Table X for a Hamada-Johnston choice for J. Also, the results of this extrapolation depend on the, so far, arbitrary choice of b. We have examined the dependence on b for a one-pole G and Hulthén J and find an uncertainty of order 0.01 in G_{ES} due to an uncertainty of order unity in b.

Table X shows that our determination of G_{ES} in our chosen time-like region is *relatively insensitive* to the choice of J. In fact, Eq. (5) shows that the value of $\mathrm{Im}Y$ in the region of Eq. (3) should be *independent* of the choice of J, as long as J obeys Eq. (6). The above sentence is true in an ideal situation, but is not true in a practical sense when we extrapolate data with statistical errors. We have examined this question by using a J with the same anomalous threshold, and the same $\mathrm{Im}J$ in region (3). We use a wave function $\exp(-\alpha r)/r$, normalizing J according to Eq. (6). Then $J(0)=(1-\alpha\rho)^{-1}$ is far from unity, and also $J-1$ is large in the region of negative t where we evaluate Y. Thus, $Y(t)$ is large for $t\leq 0$. When we extrapolate this Y, allowing it to become complex at t_A, it tends to have a large imaginary part in the region of Eq. (3), even though its imaginary part should be identical to the small values for Y based on Hulthén or Hamada-Johnston choices of J. If we used a Fourier series (A4) with a *very* large number of terms, we could recover the desired small value of $\mathrm{Im}Y$; but we are unsuccessful with a Fourier series truncated at a small value of N. We conclude that it is highly desirable to have $J(t)=1$

TABLE X. Output values for isoscalar nucleon form factor. The isoscalar nucleon form factor G_{ES} is determined from electron-deuteron elastic scattering using Eq. (9) with different choices for the quantities G and J. See Tables VII and IX.

		Two-pole G				One-pole G			
ξ (deg)	t(F^{-2})	Hulthén J		Hamada-Johnston		Hulthén J		Hamada-Johnston	
		G_{ES}	Error	G_{ES}	Error	G_{ES}	Error	G_{ES}	Error
8	0.88	0.54	0.01	0.55	0.001	0.54	0.01	0.55	0.001
26	1.04	0.56	0.03	0.57	0.002	0.55	0.02	0.57	0.002
47	1.54	0.62	0.01	0.60	0.003	0.62	0.01	0.60	0.003
66	2.33	0.70	0.02	0.64	0.002	0.72	0.02	0.65	0.002
83	3.60	0.78	0.04	0.72	0.001	0.82	0.04	0.75	0.001
90	4.27	0.81	0.04	0.77	0.001	0.86	0.03	0.81	0.001

at $t=0$, so that Y is zero at $t=0$, and Y is small for negative t.

A similar discussion applies to our sensitivity to the choice of G. It is clear that (provided $R\equiv 0$) the best possible choices for J and G would be such that $J\equiv D$ and $G\equiv 2G_{ES}$, so that Y would be identically equal to zero both for space-like and time-like momentum transfers. We guess that use of a Hamada-Johnston J and a two-pole G comes closest to this ideal condition, so we shall emphasize these values of G_{ES} below.

IV. ANOTHER EXTRAPOLATION FOR G_{ES}

We now examine two questions: (i) Are the values of G_{ES} for space-like momentum transfer of Table I consistent with the values of G_{ES} of Table X in the time-like region (3) found above from elastic electron-deuteron scattering? (ii) If they are consistent, what is the spectral function found by extrapolating the combined data to time-like regions of momentum transfer above the normal isoscalar threshold?

As shown in Fig. 2, and discussed above, previous analyses confined to negative t gave a negative answer to our first question. We here examine the consistency question by using as input data a combination of the electric isoscalar nucleon form factors for space-like momentum transfer from Table I with those given in Table X for the time-like region (3). We choose the results in Table X for a two-pole G, with two different choices for J. For Hulthén J, we use the statistical errors as given in Table X; for a Hamada-Johnston J, we arbitrarily take constant errors of 0.01. As above in our fits to G_{ES}, we use $t_0=9$ squared pion masses, and $b=2$. We use the static value and (A6) as two constraints on our least-squares fit with polynomials in η. Table XI gives the goodness of fit for different degrees N of the polynomials. The data for negative t only was fitted well by a quartic ($\phi=1.08$, given in Table II), while now a quartic gives ϕ values of 2.1 and 2.64 for Hulthén and Hamada-Johnston choices, respectively. However, if we go to higher N, we can fit the combined data with a sextic, obtaining values of 1.28 and 1.22, respectively, for our two choices of J. We interpret this behavior shown in Table XI as evidence for consistency of the two sets of data: It is reasonable to expect to use a somewhat higher value for the degree N of the polynomial when we make a substantial increase in the range of the input data, as we do by including the results of Table X. If the two sets of data were really inconsistent, one could still obtain a good fit with a polynomial in η, but only by going to a quite high value of N so that the polynomial could wiggle in a sufficiently complicated manner to accommodate itself to the inconsistency. In choosing $N=6$ for the combined data, we argue that we have not gone to a "quite high value": In particular, the number of degrees of freedom is still quite large—actually larger for our sextic fit than for our earlier quartic fit to the data of Table I.

Table XII gives the coefficients, and diagonal errors for our sextic fit. Figure 5 shows the input data, and statistical errors, and also shows our sextic fit for G_{ES} for real η. The triangles for the data from Table I, and the circles for the data of Table X, appear not inconsistent with each other. The relatively high order of six for our sextic fit seems to be demanded mainly by the unusually large range in η of our data, rather than by any marked inconsistency between the data

TABLE XI. Goodness of fit versus degree of polynomial. The goodness of fit is given by $\phi=\chi^2/$(degrees of freedom). The data of Tables I and X for G_{ES} are fitted by polynomials in η, with two constraints.

N	ϕ (Hulthén J)	ϕ (Hamada-Johnston)
2	22	39
3	4.0	3.0
4	2.1	2.64
5	2.2	1.8
6	1.28	1.22
7	···	1.13

TABLE XII. Coefficients to two-constraint polynomial fits to G_{ES} from Tables I and X.

	Hulthén J		Hamada-Johnston	
n	a_n	Error	a_n	Error
0	0.238	0.011	0.240	0.011
1	0.416	0.055	0.553	0.041
2	0.699	0.186	0.627	0.178
3	2.591	0.707	0.901	0.538
4	−3.478	0.716	−1.976	0.391
5	−2.633	0.684	−1.089	0.522
6	2.916	0.681	1.473	0.430

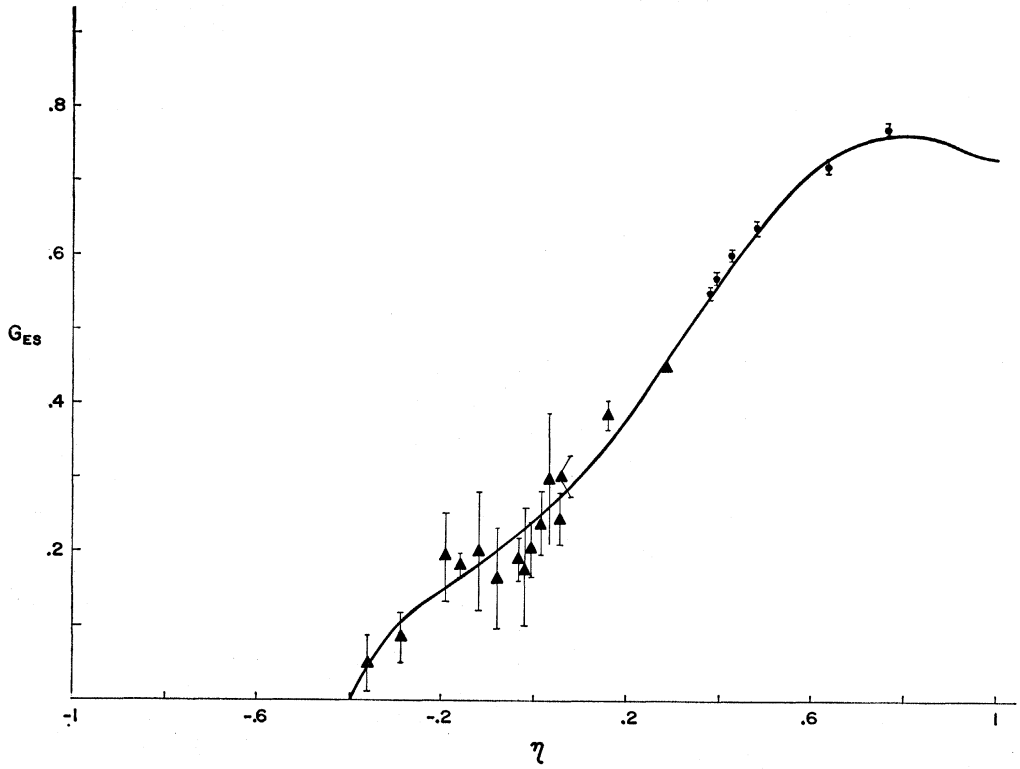

FIG. 5. The electric isoscalar form factor G_{ES} versus η. The triangles show the input data of Table I for space-like momentum transfer; the circles show our results of Table X for time-like momentum transfer (Hamada-Johnston, two-pole G); and the curve shows a sextic in η.

represented by triangles and circles. We have not shown the behavior of the sextic fit for $\eta<-0.4$: the curve dips below the axis to a minimum of -0.3, but it is never more than two standard deviations below the axis, so this extrapolation giving negative isoscalar form factors for large space-like momentum transfers is not really firm.

TABLE XIII. Another extrapolation for isoscalar spectral function (spectral functions using the coefficients of Table XII).

ξ (deg)	Mass (MeV)	Hulthén J g_{ES}	Error	Hamada-Johnston g_{ES}	Error
0	420	0.00	0.00	0.00	0.00
14.9	434	−0.31	0.08	−0.17	0.04
25.8	462	−0.93	0.28	−0.53	0.14
37.3	506	−0.20	0.25	−0.15	0.10
47.5	560	2.62	0.40	1.44	0.29
58.1	627	5.85	1.04	3.40	0.63
66.1	688	6.59	1.18	4.07	0.65
74.6	764	4.43	0.78	3.23	0.40
83.3	856	−0.61	0.69	0.78	0.62
89.9	933	−4.55	1.38	−1.30	1.06
96.1	1024	−7.63	1.95	−3.07	1.35
104	1136	−8.62	2.05	−3.89	1.31
106	1200	−8.08	1.87	−3.80	1.15
114	1354	−4.92	1.09	−2.58	0.59
122	1556	−0.04	0.55	−0.40	0.54
129	1826	4.48	1.34	1.76	1.10
134	2000	5.89	1.62	2.47	1.25
138	2211	6.48	1.70	2.82	1.27
142	2470	6.21	1.58	2.77	1.14
147	2800	5.19	1.29	2.36	0.91
151	3231	3.66	0.88	1.70	0.60
155	3818	1.94	0.45	0.94	0.28
160	4666	0.39	0.11	0.23	0.08
164	6000	−0.70	0.24	−0.27	0.20
168	8400	−1.16	0.33	−0.50	0.26
180	∞	0.00	0.00	0.00	0.00

Our arguments, from Table XI and Fig. 5, for consistency between the two types of data for the electric isoscalar form factor are clearly not rigorous. However, we believe we have shown at least that the two sets of data are not definitely inconsistent with each other: i.e., it is possible to interpret elastic electron-deuteron scattering to give isoscalar form factors not inconsistent with those given in Table I.

The spectral functions g_{ES} for two different extrapolations (based on our two choices for J) are given in Table XIII, and the Hamada-Johnston result is shown in Fig. 6. We see that either choice of J gives the first peak in the isoscalar spectral function at about 700 MeV. The same peak is seen in the quartic fit (Table V) to the data of Table I, alone. The peaks for the sextic are about as narrow ($\sim 30°$) as they could be for fits to an arbitrarily narrow resonance. The dip at 1150 MeV shown for the Hamada-Johnston result is only three standard errors below the axis; the extrapolation using the results of a Hulthén J show a four-standard-error dip at the same location. One is tempted to regard this dip as real and to associate it with the ϕ resonance at 1020 MeV; but the statistical errors are uncomfortably large. In I, Fig. 11(b), we showed that a spectral function consisting of two peaks of opposite sign would, if resolved by a truncated Fourier series, appear as two peaks spread further apart than their true positions.

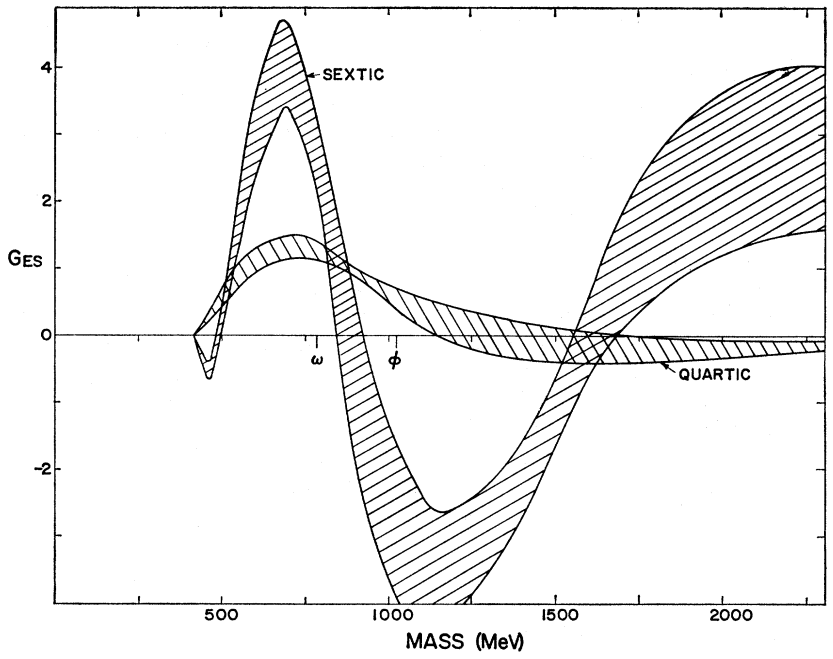

FIG. 6. The electric isoscalar spectral function g_{ES} versus mass in MeV. The quartic fit is taken from Table V, and the sextic fit from Table XIII.

Thus our values of 700 and 1150 MeV in Fig. 6 are not inconsistent with the 790- and 1020-MeV values for the ϕ and ω resonances, respectively.

We note that Bronzan and Low[12,14] have recently introduced a new selection rule they denote as A parity. From their selection rule, the ω resonance should not contribute to the isoscalar form factor. However, both of our fits to G_{ES} shown in Fig. 6 *do* show a strong peak in the region of the ω resonance; and the G_{MS} of Table V shows a similar behavior. Thus the Bronzan-Low selection rule does not hold for isoscalar form factors.

We doubt if the positive peak around 2200 MeV has any significance: It is only a two-standard-error effect, and our extrapolation method has a tendency to produce spurious peaks, as illustrated in I, Fig. 9.

V. DISCUSSION

We have extrapolated isovector and isoscalar form factors, as determined from electron-proton scattering and electron-deuteron inelastic scattering, to determine the isovector and isoscalar spectral functions. Both magnetic and electric isovector spectral functions peak around 600 MeV, or somewhat below the 750-MeV peak of the ρ resonance. A similar result was found for proton form factors in I and II. Perhaps, as argued by Ball and Wong,[15] the effective position of the resonance is shifted towards lower energies for form factor calculations, as compared to its position in two-pion final states. Alternatively, one could question whether the difference between 600 and 750 MeV is of statistical significance. A third possibility, which we plan to explore, is that one could fit isovector form factors, assuming the position and width of the ρ resonance as known from other experiments, and extrapolate the remainder of the isovector form factor to find the isovector spectral function above the ρ resonance. (We should remark here that the ρ resonance is sufficiently broad, and sufficiently strong, that it swamps any low mass contributions due to noncorrelated pion pairs.[16])

We conclude that the ρ resonance does indeed play a major role in the isovector electromagnetic nucleon form factors, but that we have not determined whether this resonance is shifted towards lower energy. The region above the ρ resonance is virtually unknown, but we can at least state that we see no strong evidence for a vector ρ' resonance, for example, that used by Freund *et al.*[17]

The isoscalar form factors, determined from the above data, extrapolate to give spectral functions peaking at 700 MeV, or slightly below 790 MeV for the ω resonance. There is weak evidence for a dip around 1600 MeV.

We are able to interpret the electric form factor G_{Ed} in elastic electron-deuteron scattering so as to be consistent with the isoscalar form factor G_{ES} found from inelastic electron-deuteron scattering and from scattering of thermal neutrons. Our interpretation assumes that either the customary Hamada-Johnston form factors are not accurate at $q^2 \approx 5$ F^{-2} and/or that appreciable nonadditive effects are present in this region.

[14] J. B. Bronzan and F. E. Low, Phys. Rev. Letters **12**, 522 (1964).
[15] J. S. Ball and D. Y. Wong, Phys. Rev. **130**, 2112 (1963).
[16] G. F. Chew, R. Karplus, S. Gasiorowicz, and F. Zachariasen, Phys. Rev. **110**, 265 (1958).
[17] A. P. Balachandran, P. G. O. Freund, and C. R. Schumacher, Phys. Rev. Letters **12**, 209 (1964).

Using our analysis of electron-deuteron elastic scattering, we find G_{ES} over a much larger range. Our extrapolation gives an isoscalar spectral function with a peak and a dip which one can identify with the ω and ϕ resonances. The Bronzan-Low selection rule fails to eliminate the effect of the ω resonance.

ACKNOWLEDGMENTS

We are grateful to D. Benaksas, K. Berkelman, J. R. Dunning, R. Hofstadter, and P. Stein for giving us unpublished experimental results. We further thank R. F. Peierls and the staff of the Cornell computing center for help in the computations and M. Casper for his determination of some of the values for G_{Ed} used in Table VII. Finally, we thank F. Gross for proposing the use of Eq. (5), for pointing out errors in other attempts of ours to analyze elastic electron-deuteron scattering, and for his criticisms of this manuscript.

APPENDIX

The form factor $G(t)$ is related to the spectral function $g(t)$ using a subtracted dispersion relation

$$G(t)=\frac{1}{\pi}\int_{t_0}^{\infty} g(t')dt'/(t'-t)+G(-\infty). \quad \text{(A1)}$$

The threshold t_0 is 4 squared pion masses (or 2.0 F^{-2}) for isovector form factors, and 9 squared pion masses (or 4.5 F^{-2}) for isoscalar form factors. We use measurements of $G(t)$ for negative t to find the imaginary part of the complex $G(t)$ for $t>t_0$ by making the conformal transformation

$$\eta=[b-(1-t/t_0)^{1/2}]/[b+(1-t/t_0)^{1/2}]. \quad \text{(A2)}$$

The choice of the parameter b is discussed at some length in I and II; throughout this paper we choose $b=2$.

We fit the values of $G(t)=K(\eta)$ with a truncated power series and determine the coefficients a_n and their error matrix:

$$K(\eta)=\sum_{n=0}^{N} a_n\eta^n. \quad \text{(A3)}$$

The order of N of the polynomial chosen is determined by statistical criteria. We examine the dependence of $\phi=\chi^2/(\text{degrees of freedom})$ on N. Usually, $\phi(N)$ levels off rather abruptly at a value near unity. We choose the degree of polynomial where ϕ is just leveling off.

The spectral function is determined using the coefficients a_n:

$$g(t)=\mathrm{Im}G(t)=\sum_{n=1}^{N} a_n \sin n\xi(t), \quad \text{(A4)}$$

where the angle $\xi(t)$ in the η plane is given by

$$\cos\xi(t)=(b^2+1-t/t_0)/(b^2-1+t/t_0). \quad \text{(A5)}$$

The complete error matrix is used to determine the statistical error in $g(t)$; we give the diagonal part of the error matrix as an indication of the errors in the coefficients.

We usually use two constraints on the coefficients: (i) that we obtain exact agreement with the static form factor, at $t=0$; (ii) that the spectral function have zero slope at threshold, namely,

$$\sum_{n=0}^{N} na_n=0. \quad \text{(A6)}$$